OBSERVATION OF LASER-INDUCED MICROSCALE VORTEX RING INTERACTIONS ON VAPORIZING METAL SURFACE

STJEPAN LUGOMER

Rudjer Bosković Institute, Bijenička 54, 10001 Zagreb, Croatia

Laser-induced microscale vortex rings have been generated on vaporizing tantalum surface, and their reconnection was studied in the presence of shock waves on the nanosecond time scale. A rich spectrum of the ring structures was obtained, some of which have been observed for the first time. Qualitatively, three classes of interactions are distinguished on the basis of relative relation of the shock momentum P_s and momentum of the circulating fluid P_c: interactions in the presence of low momentum shock waves $(P_s < P_c)$, of the shock waves with a momentum comparable to the momentum of the circulating fluid $(P_s \approx P_c)$ and of the shock waves with a momentum larger than momentum of the circulating fluid $(P_s > P_c)$.

1. Introduction

An original method has been developed to generate, observe and study vortex filaments.

The study of laser-metal interactions [1] at high energy density and short time scale (at the transition from the planar vaporization regime to the local volume boiling) has shown the generation of vortex rings and other types of knotted and unknotted vortex filaments. Vortex rings are generated by subsurface microexplosions of bubbles in the zones of volume boiling (inside the planar vaporization area), as described in Ref. 1.

This work presents continuation of the study of the vortex-ring interactions, especially of the vortex ring reconnections on nanosecond time scale, on refractory metals. Vortex-ring reconnections have been studied intensively from both theoretical and experimental point of view. Theoretical approach is generally based on the Biot-Savart model of vortex filaments which provide initial conditions for a finite difference scheme for the incompressible Navier-Stokes equation [2].

Two vortex rings, free to move come into contact and merge into a single ring, are called vortex connection. The vortex ring may then split to form the new vortex rings what is called reconnection [3]. Such interactions are difficult to be produced experimentally, and in principle they are limited to the jets and to a brief discharge of fluid from an orifice [4].

However, in laser-metal interactions, they appear spontaneously [1], and, because of ultrafast cooling alter the pulse termination, they stay frozen permanently, thus enabling a posteriori analysis.

Vortex-ring generation and their interactions due to the action of a Gaussian beam; consequently, their population, dynamics, etc., are different near the center and near the perifery of the interaction space. They appear on the ns time scale, and the question of their control (possibly by the variation of the λ-scale, τ-scale, or possibly by the variation of TEM-mode structure) is presently not known.

A Q-switched Nd:YAG laser of $Q \approx 10^7$ W/cm^2, of the pulse duration $\tau = 10$ ns and of the spot size $2d = 3$ to 4 mm, was used for the generation of vortex rings. Tantalum samples of $1 \times 1 \times 0.05$ cm in size were mechanically polished and cleaned with alcohol. The surface analysis was done by optical and scanning electron microscopes.

Approaching motion of the vortex rings to each other may be caused by the Biot-Savart law, as assumed in numerical simulations of Oshima and Izutsu [5], Kida et al. [3], Pumir and Kerr [6], and Asthurst and Meiron [2], but also by the surface shock waves what is a dominant case in laser-material interactions. Laser-generated shock waves travel from the center of the spot toward it's periphery, from the periphery toward the center, and also between front and back side of the sample [7]. Their constructive interference at one point and destructive at the other point, dispersion on imperfections of the solid material etc., cause the turbulence of the molten metal surface. They give rise to an inhomogeneous shock-wave field with strong influence on the vortex-ring dynamics and mutual interactions of vortex rings. Vortex ring interactions are inhomogeneous and belong to different classes that are present in various regions of the spot. Their classification is based on the relative relation between momentum of the circulating fluid, P_c, and momentum of the shock wave, P_s (it may also be expressed by the relative relation of the circulation, and the shock velocity, Γ and M, respectively). Qualitatively, we distinguish the class of interactions in the presence of the low momentum shocks or in their absence $(P_s < P_c)$, the class of interactions in the presence of the shock waves of momentum comparable to the momentum of the circulating fluid $(P_s \approx P_c)$ which disturbs the reconnection process by deforming the vortex; and the class of interactions in the presence of high momentum shock waves $(P_s > P_c)$ which cause breaking of the cross-linked rings.

2. Vortex rings with $P_{shock} > P_{circulating\,fluid}$

The cross-linking interaction of two vortex rings follows the scenario described by Fohl and Turner [4] based on experimental observations and by Kida et al. [3] and Oshima and Izutsu [5] based on the numerical simulations.

Two ring vortices are located in close viscidity at an angle (Fig. 1). The vorticity is distributed parallel to the centerlines of the vortex rings and distributed counterclockwise for one ring and clockwise for the other one. Within each cross-section, vorticity is given by the Gaussian form [3]:

$$\omega(r) = \omega_0 \exp(-r^2/\sigma^2), \tag{1}$$

where r is the distance from the core center, and ω_0 and σ (core size) are constants. The circulation Γ of each ring is equal to $\pi\omega_0\sigma^2$ [3]. Reconnection of two rings has many stages which have been visualized in the numerical simulations of Kidda et al. [3] Oshima and Isutzu [5] and of Asthurst and Meiron [2]. The reconnection can hardly be observed experimentally, and experimental evidence of this process and its stages are really very rare. Our observations of the reconnection process in laser-matter interactions show not only its various stages, but also some new situations in the ring–ring interactions, not reported previously.

Vorticity of two rings that enter the reconnection process (the initial phase) is always opposite. In the second phase (the stage a-c according to Kidda et al. [3]), when the bridge between two rings is formed, the topological rearangement associated with the rearrangement of vorticity occurs.

The following micrographs show the vortex rings in various stages of the reconnection, reached in the moment of the pulse termination.

Figure 1a shows the inital phase of reconnection when two rings touch each other. They disappear at the touching point by annihilation of vorticity of opposite sign. Then follows merging of two rings into a single distorted ring by cut and connect [3,5].

Figure 1b shows the second phase of reconnection scenario when the vortex tube with saddle profile is formed with increased radius of curvature. The two antiparalel portions of the saddle approach each other as they are straightened [3,5]. As they become straight, their approach is stopped before their contact is established. Another reconnection process happens at this moment; new "bridges" appear on the front side of the vortex tube at the border between the straight and circular parts of the tube. As a result, the merged vortex tube changes topologically into two rings connected by two "legs", what represents the third phase of the reconnection scenario. The cross-linked rings seen in Fig. 1c can be attributed to the third phase with the bridges on the rings established, and with the leg-tubes significantly straightened.

More complex structures, also corresponding to phase 3, consisting of two knotted rings cross-linked with the third one, can be seen in Fig. 1d. This structure (observed for the first time) represents a ring with the Hopf bifurcation cross-linked with the other ring. It indicates the chain of events which are time-ordered. Time
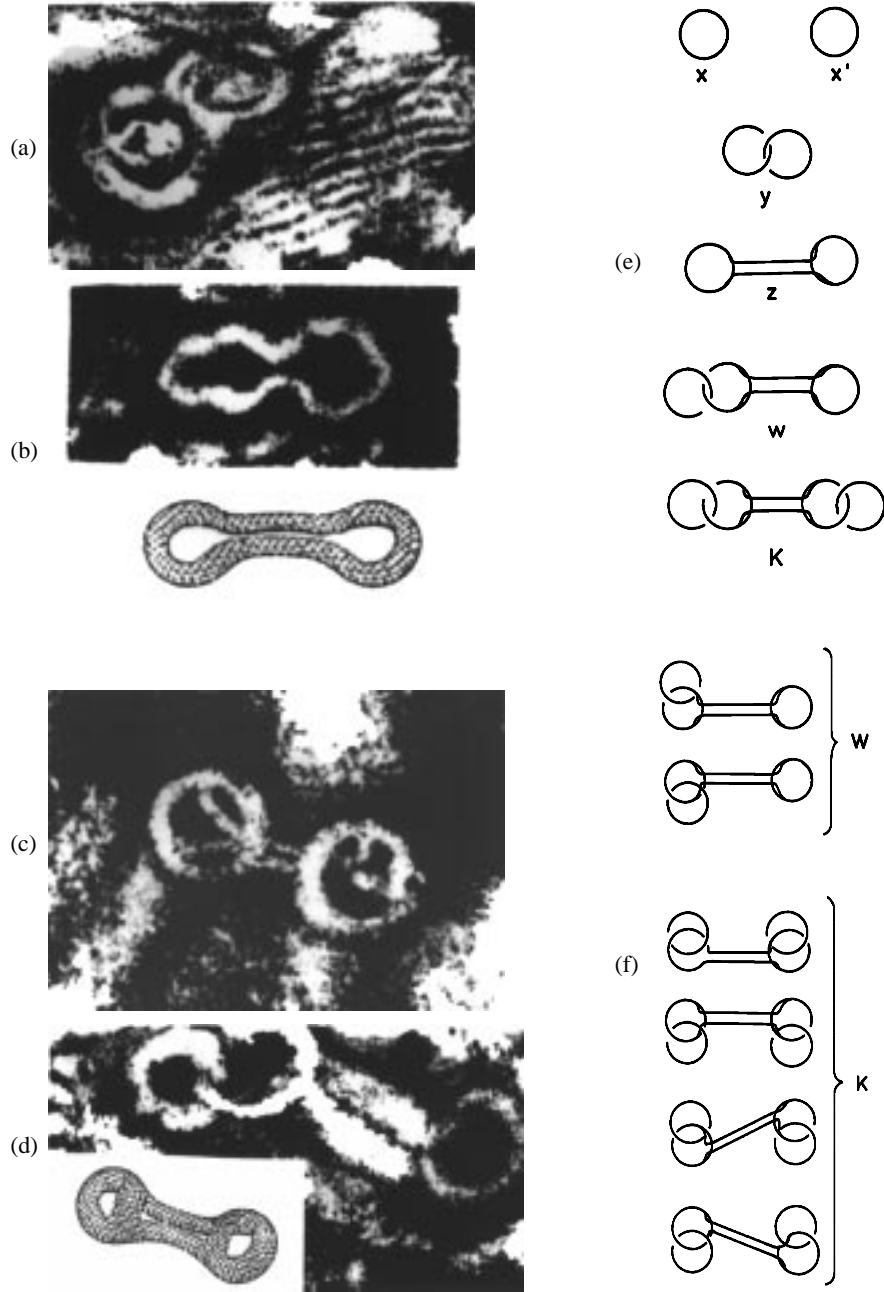
Fig. 1 (at left). Reconnection of two vortex rings on liquid Ta *surface without presence of the shock waves. a) Two rings at the moment of touch. Magnification, $M = 2300\times$. Numerical filtering reveals thinning of the rings around the touching point, which corresponds to the initial phase of reconnection; b) Two rings after the first reconnection, which corresponds to the second phase of reconnection. $M = 1600\times$. (The corresponding numerically generated form is given for comparison (from Ref. 5)); c) Two rings after the second reconnection, corresponding to the third phase of reconnection. $M = 600\times$. Long stretched leg-tubes are clearly seen; d) Two rings with the Hopf link, cross-linked with the third one, corresponding to the phase 3 of reconnection. Flattening of both leg-tubes indicates diffusive spreading and the core deformation because of interaction with the background fluid. (The corresponding numerically generated form is given for comparison (from Ref. 5)); e) Schematic representation of the states X, Y, Z, W and K; f) Twofold and fourfold degenerate states W and K defined by the number of possible cross-linkings.*

ordering relates to the fact that the vortex ring must first bifurcate generating the Hopf link (knotted knot) [1], and then it may establish the cross-linking with another ring in it's vicinity (the reverse process is not possible for purely topological reasons). This indicates that the fastest process, which occurs first, has a lower order of complexity, and then follows a slower one of a higher order of complexity. Thus, the ordering is twofold: according to the increasing order of topological complexity and according to decreasing process rate.

We introduce the assumption that the above processes may be symbolically described as follows: we assume the ring configurations to be the states denoted X, Y, Z, W and K, as is schematically shown in Fig. 1e. The states X and X' correspond to the clockwise and counterclockwise vorticity and can be represented by 3×3 matrices $\mathbf{X}$ and $\mathbf{X}'$, respectively [9]:

$$\mathbf{X} = \begin{pmatrix} 1 & 0 & 0 \\ 0 & 1 & 0 \\ 0 & 0 & 1 \end{pmatrix} \quad \text{and} \quad \mathbf{X}' = \begin{pmatrix} 0 & 0 & -1 \\ 0 & -1 & 0 \\ -1 & 0 & 0 \end{pmatrix}. \tag{2}$$

The state Y is a Hopf link represented by the matrix

$$\mathbf{Y} = \begin{pmatrix} 1 & 0 & -1 \\ 0 & -1 & 0 \\ -1 & 0 & 1 \end{pmatrix}.$$

It can be obtained from the state X by the operation

$$\mathbf{Y} = \mathbf{O}_1 \mathbf{X}, \quad \text{where } \mathbf{O}_1 \text{ is the operator} \quad \mathbf{O}_1 = \begin{pmatrix} 1 & 0 & -1 \\ 0 & -1 & 0 \\ -1 & 0 & 1 \end{pmatrix}. \tag{3}$$

The state Z (corresponding to the cross-linked rings of clockwise and counterclockwise vorticity), is represented by the matrix:

$$\mathbf{Z} = \begin{pmatrix} 1 & 0 & 1 \\ 0 & 0 & 0 \\ 1 & 0 & 1 \end{pmatrix}$$

and obtained by the operation

$$\mathbf{Z} = \mathbf{O}_2\left(\mathbf{X}\cdot\mathbf{X}'\right), \quad \text{where} \quad \mathbf{O}_2 = \begin{pmatrix} -1 & 0 & -1 \\ 0 & 0 & 0 \\ -1 & 0 & -1 \end{pmatrix}. \tag{4}$$

The states X, Y and Z are the basic states, while W and K are the combined states obtained by the action of the operators $\mathbf{O}_1$ and $\mathbf{O}_2$ on the matrices $\mathbf{X}$ and $\mathbf{X}'$:

$$\mathbf{W} = \mathbf{O}_2\left[(\mathbf{O}_1\mathbf{X})\,\mathbf{X}'\right] = \begin{pmatrix} -2 & 0 & 2 \\ 0 & 0 & 0 \\ -2 & 0 & 2 \end{pmatrix} = 2\begin{pmatrix} -1 & 0 & 1 \\ 0 & 0 & 0 \\ -1 & 0 & 1 \end{pmatrix} \tag{5}$$

and

$$K = \mathbf{O}_2\left[(\mathbf{O}_1\mathbf{X})\cdot(\mathbf{O}_1\mathbf{X}')\right] = \begin{pmatrix} 4 & 0 & -4 \\ 0 & 0 & 0 \\ -4 & 0 & 4 \end{pmatrix} = 4\begin{pmatrix} 1 & 0 & -1 \\ 0 & 0 & 0 \\ -1 & 0 & 1 \end{pmatrix}. \tag{6}$$

Factors 2 and 4 in Eqs. (5) and (6) indicate the existence of two and four equivalent states, W and K, respectively. These degenerate states are established by different combinations in the ring connection, as shown in Fig. 1f. Notice that the states W and K can only be generated by the order of operations as given in Eqs. (5) and (6), respectively, confirming the time ordering. The change of the order, i.e., $\mathbf{W} = \mathbf{O}_1\left[(\mathbf{O}_2\mathbf{X})\,\mathbf{X}'\right] = \mathbf{O}_1\mathbf{Z}$ is excluded, since $\mathbf{O}_1\mathbf{Z} = 0$, what is an argument in favour to the conclusion about time ordered processes based on topological arguments.

3. Vortex rings with $P_{shock} \approx P_{circulating\,fluid}$

Deformation before cross-linking: Low intensity shock waves may cause deformation of one or both rings by circumferential core deformation, what, according to Widnal and Sullivan [8], is a three-dimensional sinusoidal oscillation. (Fig. 2a). More complex case appears when one or both rings are elliptically deformed and, in addition, strongly twisted (Figs. 2b and c). Whenever torsional deformation of closely spaced ring was observed, the cross-linking did not take place. In principle, deformation of two vortex rings is a symmetry breaking process which generates the structure of the lower symmetry. In addition, it may even increase the order of topological complexity, thus changing the cross-linking process from the fast into the slow one. If this process takes longer time than the pulse duration, the cross-linking does not happen. Thus, at a given time scale, deformation of the rings suppresses their cross-linking.
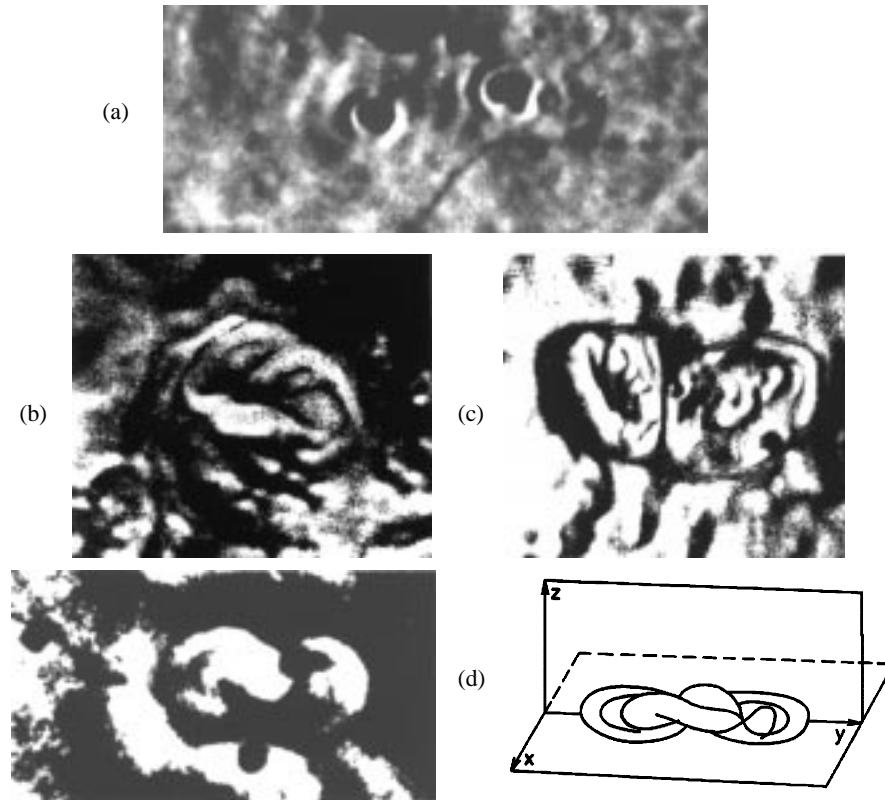
Fig. 2. Deformed vortex rings by the shock waves prior to reconnection. a) Two vortex rings (one deformed by 3D circumferential oscillation) approach each other. $M = 1100\times$; b) One twisted and elliptically deformed vortex ring. $M = 1800\times$; c) Two twisted and elliptically deformed rings at a distance $d < \sigma$ (smaller than the core size) which do not undergo cross linking. Tiny sharp line separating both rings is clearly seen, $M = 1800\times$; d) Cross-linked ring with the short leg-tubes. Magnification and numerical filtering reveal that the leg-tubes are spirally wrapped as shown on the schematic illustration.

Deformation during cross-linking: An interesting type of structure (not reported previously) is shown in Fig. 2d. This structure may be attributed to the deformation that coincides with the cross-linking in the presence of a turbulent field. Two rings are cross-linked without stretching, what seems to be a characteristic of very fast reconnection at low Reynolds numbers. According to Asthurst and Meiron [2] and discussion of Pumir and Kerr [6], every fast reconnection for Reynolds numbers (defined by the ratio of the circulation divided by viscosity, Γ/ν) between 100 and 1000 occurs without stretching. Very specific characteristic of the object in Fig. 2d is the cross linking which consists of a single tube lying out of the cross-linking plane, actually in the plane perpendicular to it. However, a detailed look on the enlarged and numerically filtered micrograph indicates that the cross-linking tube is not a single one, but a pair of tubes spirally wrapped with one

or may be two spiral turns. This can not be compared with any experimental or numerically generated pattern of reconnection reported in literature. One possible comparison is possibly with the speculation of Asthurst and Meiron [2] that the reconnection may occur in a turbulent-flow field. In our case, the turbulent field (local) is caused by week shock waves. According to this speculation and a calculation done for the circulation ratio of 2:1, the two tubes are spirally wrapped. This occurs in the presence of axial flow associated with tube stretching [2]. However, the tube stretching does not occur in our case, and we doubt whether the speculation of Asthurst and Meiron [2] is (completely) applicable to the case observed.
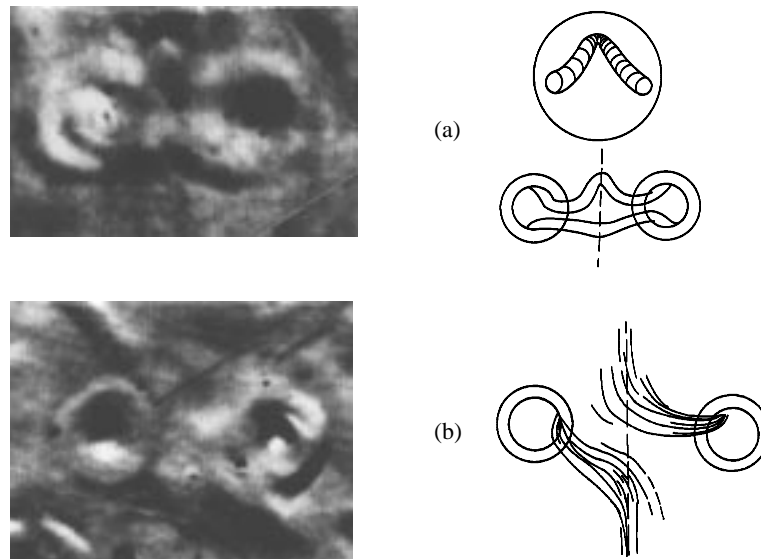

Fig. 3. Deformation of the cross-linked structure. a) Bedding of the tubular legs. $M = 2300\times$. View of the tube at the buckling point (schematically). b) Deformation (and collapse) of the tubular legs between cross-linked rings, with diffusive spreading. $M = 2300\times$. Shematic reconstruction of the process.

Deformation after cross-linking: Deformation of the vortex structures may occur if the shock wave strikes the rings after cross-linking, through the deformation of the cross-linking tubes ("legs"), what can be seen in Fig. 3a. Magnification and numerical filtering reveal that the legs connecting the rings are deformed with buckling caused by the axial compression.

The shock waves may even cause a core collapse by a large spreading of the cross-linking tubes, the "legs" (see Fig. 3b). The core spreading to about three times the initial core size takes place tangentially to the line of discontinuity, which may be assumed to be a shock front, and which is almost normal to the tube "legs". According to Erlebacher et al. [10], when the shock is in the direction normal to the vortex axis, a deceleration of the vortex, which may lead to its breakdown, takes place. A large core spreading indicates a very

fast (abrupt) deceleration of the fluid (in comparison with a slow core spreading caused by the viscous effects). The process which leads to the spreading of the core vorticity turns every vortex tube in counter direction because of their antiparalel vorticity. However, one can see that the bridges (see description of Kida et al. [3]) stay unaffected.

4. Vortex rings with $P_{shock} > P_{circulating\,fluid}$

Very strong shock waves may cause either violent motion of one ring towards the other one at rest as shown in Fig. 4a., or the acceleration of the two rings and their collision (due to the shocks from opposite sides), as shown in Fig. 4b.
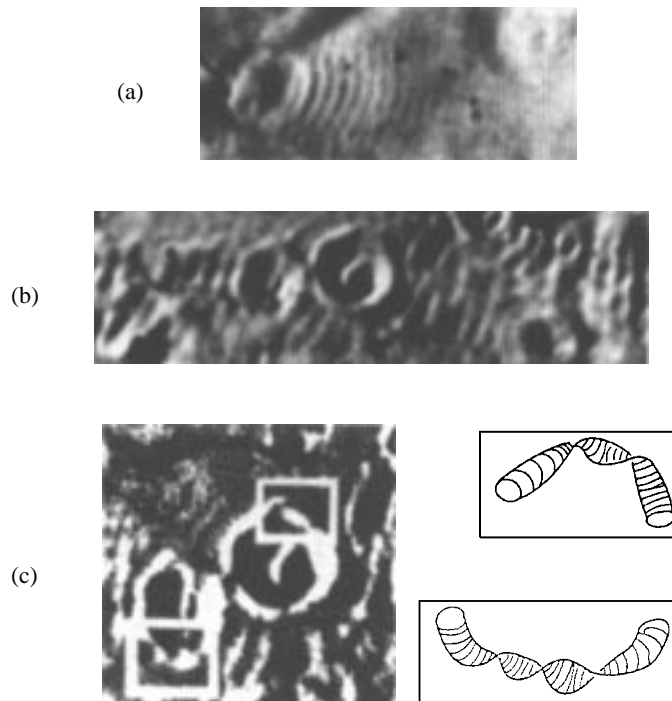

Fig. 4. Collision of two vortex rings with the strong shock waves. a) Acceleration of one ring towards another one at rest. $M = 2300\times$. b) Collision of two accelerated rings under an angle of about $23°$. $M = 1100\times$; c) Magnification and numerical filtering reveals details of the broken rings into arc segments. Schematic illustration represents the arc segments separated by nodal points of singularity.

The rings approach each other under an angle of $23°$ what, according to Fohl and Turner [4] leads to a "double ring formation", i.e., to reconnection. Since the rings collide with great velocity, this process is accompanied by a series of successive phenomena, summarized in the scenarios (i) to (v).

(i) Interaction of the rings with the shock waves opens the possibility for the momentum

transfer, and consequently for the change of the circulation, Γ, of the vorticity ω. This manifests as a core thickening, which occurs on the same (right) side of the cross-linked rings (see Fig. 4.). Similarly, the core thinning occurs on the left side of both rings (see Fig. 4). Thus, the core thickening and thinning seems to occur simultaneously on the opposite sides of the rings. Magnification and numerical filtering reveal more details of this structure (Fig. 4c).

(ii) Shortening of the cross-linking legs as a consequence of the axial compression of the shocks can be seen in Fig. 4b. These legs are much shorter than the legs of the cross-linked rings in the absence of the shock waves.

(iii) Backward reflection of the shock waves from both sides of the cross-linked rings causes a ripple pattern with characteristic phase shift (Fig. 4b).

(iv) Generation of singularities in vorticity and of the nodal shape of the core of both rings can be seen in Fig. 4b. Numerical study of the vortex ring reconnection by Asthurst and Meiron [2] have shown that the nodal shape appears through the singularity in the core vorticity. They have found that distortion of the filament only occurs over an arc which is less than 10% of the initial ring circumference. The small arc segment is frozen in time, i.e., the arc length within this region grows with a resulting reduction in the core size to conserve the vorticity volume. Then self-similar growth pattern appears in the form of modules along the filament generated at points where the axial strain is zero [2]. This type of dynamics leads to a singularity in finite time, as described by Sigia and Pumir [11].

Figure 4c indicates that the singularities in the core vorticity caused by the shock waves take place after the ring reconnection. Both rings are shrinked to zero vorticity at singular points, giving rise to a relatively small number of arc segments of vorticity. Distortion of the core is significant and occurs on all segments regardless of their length or curvature. Therefore, thickness of the segment core is not constant but varies along its length, what indicates the presence of oscillations in the core size. This further indicates that vortex ring during the interaction with the shock wave is not frozen, i.e., its core size, σ, changes in time very fast and causes that the volume vorticity is not necessary conserved.

(v) In contrast to the case studied by Asthurst and Meiron [2], Fig. 4c indicates that the real break occurs in all nodal points of both rings. Broken seqments are separated from one another and move from their position, thus disturbing the circular geometry of the rings. The largest arc segment is strongly bent towards the center on the same (right) side of both rings. This bending of the arc segment was not observed previously, neither experimentally nor in the numerical simulations.

The volume of the broken segments, V, (the fragmented vorticity volume), was determined by measurement the length of the arc segments, s, and of the core diameter, σ. Measurements of σ have been done at three positions for every segment, and the average values were used. Diagram (Fig. 5) gives the volume, V, as a function of the length of the segment s, and suggests the dependence od the type:

$$V \sim s^D, \tag{7}$$

where D is the coefficient of direction in the log-log plot: $D = 5/3 = 1.67$. The exponent, D, is the fractal dimension of the ring breaking into segments of vorticity caused by the shock waves.
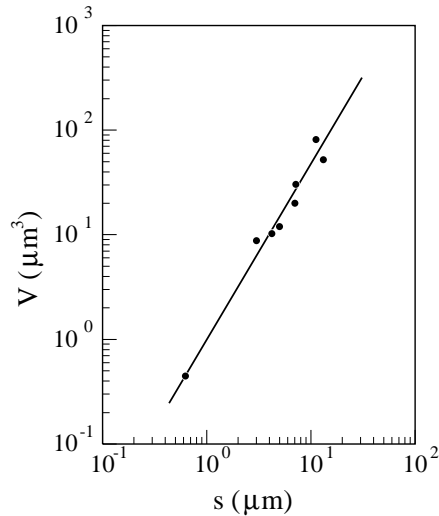
Fig. 5. Log-log plot of the volume vorticity of broken segments of the length s.

The time scale of 10 ns at which the vortex ring interactions were studied, is about 10^5 times shorter than the scale of Oshima and Izutsu [5]. To our knowledge, it is the shortest time scale reported so far. These experiments have demonstrated that complete vortex ring reconnection process may occur even on an extremely short time scale, thus positively answering the question that arose in the literature. The experiments have also demonstrated the existence of a reach spectrum of dynamical phenomena (associated with the ring reconnection), of a higher topological complexity than in the absence of the shock waves.

5. Conclusion

Vortex rings and structures generated by their interactions can be very easily produced by laser – matter interactions on short time scales. A variety of structures obtained in the ring – ring interactions (reconnections), occuring in the presence of the shock waves, have been clasified with respect to the relation between the momentum of the shock wave, P_s, and of the circulating fluid, P_c.

The matrix formalism has been introduced to describe various structures obtained as a result of the ring – ring interactions. For some complex structures, two-fold and four-fold degeneracy and time ordering of the processes were obtained. For the rings experiencing deformation (torsion), the reconnection process was shown to be delayed or even prevented, on the time scale of the laser-pulse duration.

For very strong shocks, the ring fractalization was shown to take place, with the fractal dimension of 5/3.

This study of vortex rings and their reconnection, performed on the time scale of 10 nanoseconds seems to be the first study on such a short time scale.

References

1) S. Lugomer, Phys. Rev. bf B 54 (1996) 4488; S Lugomer, J. Fluids and Structures (submitted);

2) W. T. Asthurst and D. I. Meiron, Phys. Rev. Lett. **58** (1987) 1632;

3) S. Kida, M. Takaoka and F. Hussain, Phys. Fluids **A 1** (1989) 630;

4) T. Fohl and J. S. Turner, Phys. Fluids **18** (1975) 433; A. Glezer, Phys. Fluids **31** (1988) 3532;

5) Y. Oshima and N. Izutsu, Phys. Fluids **31** (1988) 2401;

6) A. Pumir and R. M. Kerr, Phys. Rev. Lett. **58** (1987) 1636;

7) J. D. O'Keefe, C. H. Skeen and C. M. York, J. Appl. Phys. **44** (1973) 4622;

8) S. E. Widnall and J. P. Sullivan, Proc. Roy. Soc. (London) **A 332** (1973) 335;

9) More detailed theoretical consideration, which will include the symmetry of the states, the properties of determinantes of the matrices (regular for the basic states and singular for derived states), etc., will be given in a forthcomming paper.

10) G. Erlebacher, M. Y. Hussaini and C. W. Shu, *Interaction of a Shock with Longitudinal Vortex*, preprint.

11) E. D. Sigia and A. Pumir, Phys. Rev. Lett. **55** (1985) 1749.

OPAŽANJE MEĐUDJELOVANJA MIKRONSKIH LASERSKI–INDUCIRANIH VRTLOŽNIH PRSTENOVA NA POVRŠINI TANTALA

Laserski inducirani vrtložni prstenovi mikronske veličine generirani su na površini tantala. Njihova su se prespajanja proučavala pod djelovanjem udarnih valova u nanosekundnim vremenskim intervalima. Proizveden je bogat spektar struktura vrtložnih prstenova, od kojih su neki opaženi prvi puta. Kvalitativno, njihova se međudjelovanja mogu razvrstati u tri klase na osnovi impulsa udarnih valova, P_s, i impulsa cirkulirajućeg fluida, P_c: $P_s < P_c$, $P_s \approx P_c$ i $P_s > P_c$.